Bei diesem Beitrag handelt es sich um einen wissenschaftlich begutachteten und freigegebenen Fachaufsatz („reviewed paper“).

doi.org/10.37544/1436-4980-2026-03-22
Datum der Einreichung: 23.11.2025
Datum der Annahme: 15.12.2025
Datum der Veröffentlichung: 07. 04.2026

Neural operators for solving multi-physics problems in tempered glass

Artificial intelligence for simulation in glass manufacturing

T. Hussein, J. Schilp

ABSTRACT Predicting temperatures and residual stresses is essential in the glass tempering process. Classical numerical solvers are accurate but slow in large domains. This study develops a variant of a Multi-Input Fourier Neural Operator (MIFNO) as a fast surrogate, trained on FEM data. It predicts temperatures and stresses from process parameters with strong accuracy and generalization, achieving 7.7× speedup on seen cases and 15× on unseen cases.

STICHWÖRTER
Künstliche Intelligenz (KI), Simulation, Werkstoffe

Künstliche Intelligenz für Simulationen in der Glasherstellung

ZUSAMMENFASSUNG Die Vorhersage von Temperatur- und Eigenspannungen ist entscheidend im Glas-Temperprozess. Klassische numerische Löser bieten hohe Genauigkeit, sind jedoch in großen Domänen rechenintensiv. Diese Studie entwickelt eine Variante des Multi-Input Fourier Neural Operator (MIFNO) als schnelles, auf FEM-Daten trainiertes Surrogat. Das Modell berechnet Temperatur- und Spannungsfelder präzise aus den Prozessparametern und erreicht eine Beschleunigung von 7,7× bei trainierten und 15× bei untrainierten Fällen.

1 Introduction and motivation

Computational efficiency is an important aspect in modelling multi-physics problems, as it affects both numerical performance and hardware utilization. However, numerical methods show great robustness and accuracy in modelling complex time-dependent problems, while real-time simulation and high dimensional problems require massive computational times, which might extend up to days [1]. Parallelization and optimized Galerkin formulations improve performance but remain limited for high-dimensional problems [2, 3].

Data-driven AI models have recently attracted major interest from developers concerned with efficiency issues. For prediction tasks, supervised models learn from labelled data, while unsupervised methods extract patterns from unlabelled datasets [4, 5]. Physics-informed neural networks (PINNs) and their semi-supervised learning enhance prediction accuracy by incorporating PDE (Partial Differential Equations) residuals and boundary losses directly into the training objective [6, 7]. Neural operators are based on supervised learning methods, where the operation detects patterns between the labelled data. These operators show remarkable efficiency with a speedup between 25 and 1000 compared to numerical solvers [8, 9]. There are several architectures coming from these operators, such as PiNOs, FNOs, and DeepONets [10, 11].

This work develops a variant of the Fourier Neural Operator (FNO) tailored for multi-physics modelling in tempered glass. The proposed Multi-Input Fourier Neural Operator (MIFNO) maps process parameters directly to temperature and residual stress fields, enabling rapid and parameterized simulations.

Section 2 reviews the state of the art in computational efficiency and numerical modelling of tempered glass. Section 3 introduces the methodology, including data generation via Finite Element Method (FEM), the architecture of the surrogate model, and the training and evaluation workflow. Section 4 presents and validates the results through quantitative and qualitative analyses. Finally, Section5 concludes the study and outlines potential extensions toward fully data-driven process twins in glass manufacturing.

2 State of the art

Tempered glass plates have been modelled over time using different numerical methods, with varying dimensions and environmental conditions, based on viscoelasticity and Narayanaswamy models. 3D implementations with FEM, such as those in Abaqus and structural relaxation models provide accurate physical insight of tempered glass plates [12, 13]. The latter models are used in our work for generating the training data.

Recent studies apply AI models to accelerate such simulation runs, using data-driven and physics-informed paradigms. Since tempered glass simulation is governed by heat diffusion and linear elasticity equations as example of time-dependent partial differential equations, this research aims to find out an efficient solution based on these equations. PINNs have shown high accuracy for thermal and mechanical problems under different boundary conditions [14–18]. Neural operators further improve scalability by learning data-to-solution mappings for PDEs without explicit physical constraints [19–21].

Unlike neural networks, these operators require parameterization to achieve flexible and independent models without the need

to re-import input parameters and boundary conditions during operation. Several efforts have been made to parameterize neural operators, such as [22, 23]. Other examples include Multi-Input FNOs [24] and Multi-Input Operator Networks [25]. These models enable efficient, reusable solvers for various process conditions, forming the conceptual foundation of the MIFNO approach proposed in this work.

3 Methodology and AI architecture

The workflow follows a structured simulation-to-model pipeline for AI-based modelling of the glass cooling process, as shown in **figure 1**.

The governing partial differential equations for heat transfer and stress evolution are first defined and then solved using FEM simulations under varying material and process parameters. The resulting high-fidelity datasets are used to train surrogate models that learn mappings between process inputs and corresponding temperature and stress fields. The trained models are then validated against FEM reference data and then visualized through process-control tools for integration into digital factory environments.

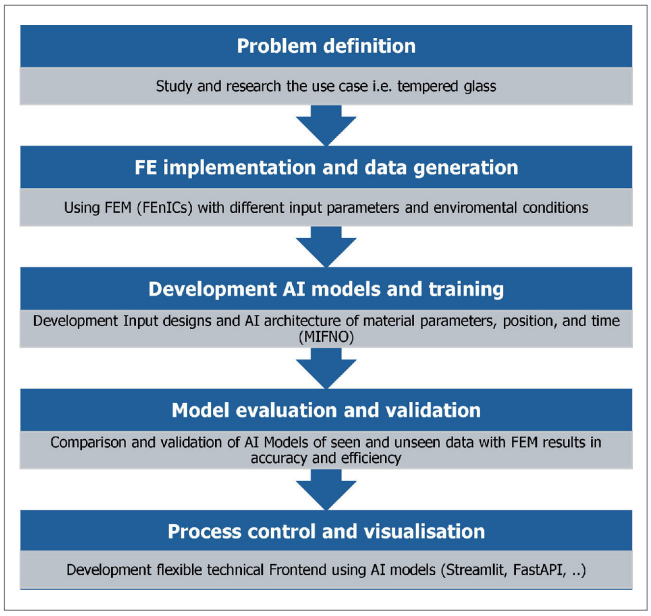

Figure 1 Workflow of the AI-based surrogate modelling framework for tempered glass cooling. *Source: Universität Augsburg*

3.1 Problem definition

The calculation of temperature profiles and residual stresses in tempered glass is based on four models, which are essential to represent its thermo-rheological behaviour during cooling process: thermal, structural relaxation, mechanical and thermo-rheological models. The calculation scheme of residual stresses is governed by partial differential equations, while other sub-models are expressed by analytical equations [12, 26].

During cooling in the tempering process, heat transfer conditions are time-dependent and represent conduction, convection and radiation from air jets into glass ribbon. The Fourier heat flow equation is incorporated into the energy balance to obtain the heat diffusion equation [27, 28]. The mechanical behaviour follows linear elasticity, and structural relaxation and thermo-rheological effects are implemented according to [12, 13].

3.2 FEM implementation and data generation

A one-dimensional (1D) mesh is constructed on Gmsh software with 49 elements (50 nodes), where the boundary conditions are represented by points on the left and right of the 1D domain. The approximation solutions are solved using FEniCSx software in variational formulation (weak form) of the heat diffusion equation considering convective and radiative heat transfer coefficients as boundary terms [29, 30], as written in equation 1.

$$\int_{\Omega}^{0}\left(\frac{\partial T}{\partial t}\right)\cdot v\,dx+\int_{\Omega}^{0}\boldsymbol{\alpha}\left(\frac{\partial^2 T}{\partial x^2}\right)\cdot v\,dx=$$

$$\int_{d\Omega}^{0}\boldsymbol{-htc}\,(T(x,t)-T_{ambient})\cdot v\,ds-\int_{d\Omega}^{0}\boldsymbol{\epsilon\sigma}\,(T(x,t)^4-T_{ambient}^4)\cdot v\,ds \qquad (1),$$

where $\forall x \in \Omega$, $\forall v \in V$ and V is the finite element function space. "$\cdot$" is dot product of two vectors, T is the temperature distribution as a function of position and time, t is time, x is the spatial coordinate, α is the thermal diffusivity, htc is the convective heat transfer coefficient, $T_{ambient}$ is the temperature of the surrounding air, ϵ is the emissivity of the surface, σ is the *Stefan-Boltzmann* constant, Ω is the spatial domain and $\partial\Omega$ is the spatial domain on the boundary.

The mechanical model is formulated using the weak form of linear elasticity, neglecting traction forces and imposing Dirichlet boundary conditions on displacement, as illustrated in equation 2.

$$\int_{\Omega}^{0}\sigma:\nabla v\,dx+\int_{\Omega}^{0}f\cdot v\,dx=\int_{d\Omega}^{0}T_{force}\cdot v\,ds \qquad (2),$$

where "$:$" represents the double dot product (or double contraction) of two tensors, σ represents the stress tensor, f is body force per unit volume, and T_{force} are traction forces, these forces are neglected. The other remaining structural relaxation and thermo-rheological models are integrated as post-processing calculations and customized as mentioned in the works [12, 26–29].

Simulations are executed on "Apple M1 Pro system" (1 active core on CPU, 16 GB RAM), requiring 0.69 s to compute temperature and stress fields over 50 s of simulated cooling. Sixteen parameterized process cases are generated from the governing equations to form the training dataset for the surrogate model, as shows **figure 2**. An extended study with 81 cases is also performed.

3.3 Model architecture and training

The architecture of the proposed AI-based surrogate model is inspired from Fourier Neural Operators (FNO), DeepONet, and Multi-Input Fourier Neural Operators (MIFNO) [22–25]. It combines the spectral efficiency of FNOs with the multi-parameter flexibility of MIFNOs to map process parameters directly to full spatial-temporal field predictions. N represents the number of use cases/samples, N_x represents the number of spatial discretization points along the glass domain (e.g., mesh nodes or finite elements) and N_t is number of temporal discretization steps in the simulation time. **Figure 3** illustrates the model architecture, which includes four main stages:

Parameters	Case 1	..	Case 16
Convective heat transfer co. (htc)	100	..	200
Emissivity (ϵ)	0.7	..	0.85
Stefan Boltzmann constant (σ)	2e-8	..	6e-8
Thermal diffusivity (α)	5	..	20

Parameters	Case 1	..	Case 16
Temperatures (T)	[870,]	..	[850,]
Stresses (σ)	[0.7,]	..	[1.5,]

Figure 2 Overview of 16 parameterized simulation dataset used for training the surrogate model, showing process input parameters and their corresponding temperature and stress outputs. *Source: Universität Augsburg*

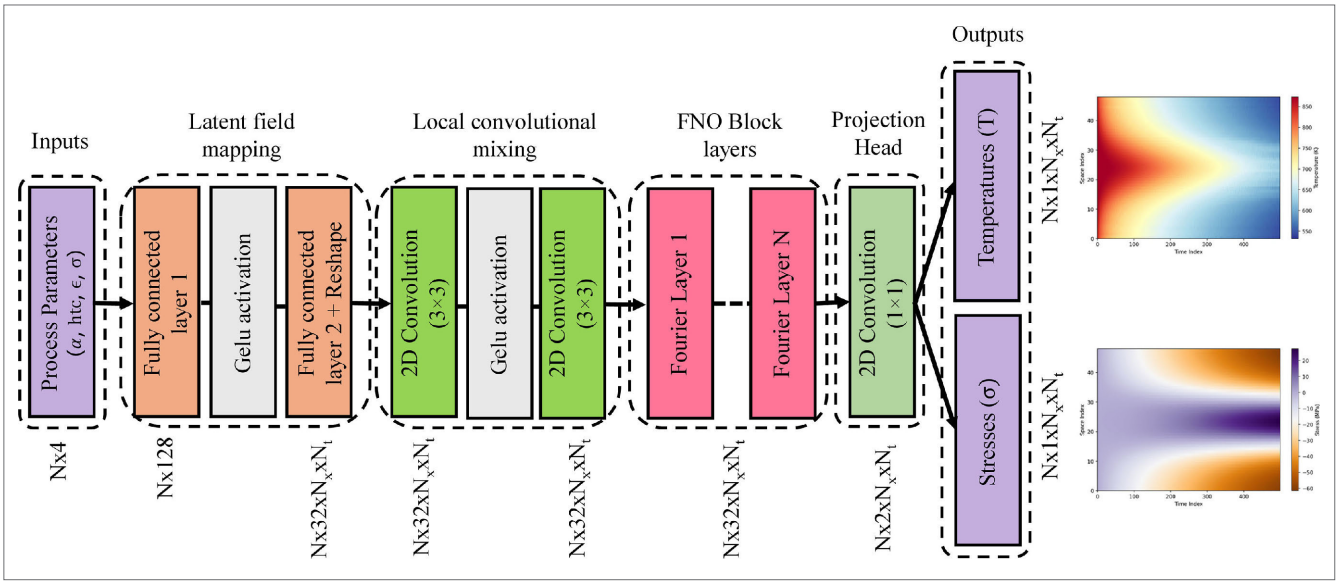

Figure 3 A variant from Multi-Input Fourier Neural Operator (MIFNO) architecture for predicting temperature and stress fields from process parameters in tempered glass cooling [24]. *Source: Universität Augsburg*

1. Input Encoding and Latent Field Mapping – Process parameters (e.g., *htc*, ϵ, α, σ) are mapped through two fully connected layers to form a latent representation of the domain.
2. Local Convolutional Mixing – Two 2D convolution layers (kernel size 3×3) with GELU activation locally refine spatial–temporal dependencies in the latent field.
3. Fourier Operator Layers – Multiple spectral convolution blocks perform global transformations in Fourier space to efficiently capture long-range dependencies.
4. Projection Head and outputs – A 1×1 convolution reduces the feature dimension to two output channels, representing temperature (T) and residual stress (σ) distributions.

Training is performed on Apple M1 Pro system (8 active cores on CPU, 16 GB RAM). Each forward pass completes 0.09 s per sample on trained parameters and 0.046 s on unseen cases, generating temperature and stress profiles for 50 s of simulated cooling. The model is optimized using the Adam optimizer with a learning rate of 0.001, trained over 1000 and 2000 epochs, ensuring convergence across both small (16 cases) and extended (81 cases) datasets.

3.4 Model evaluation and validation

The surrogate model is quantitatively evaluated using the relative L² error metric and validated against the reference FEM solutions for both temperature and residual stress fields. A dual-output loss function is defined as a weighted combination of the mean-squared errors (MSE) of temperature and stress predictions, as shown in equation 3.

$$\mathcal{L}_{total} = \omega_T \mathcal{L}_T + \omega_S \mathcal{L}_S \quad <3>$$

The loss functions of each prediction are described in equation 4.

$$L_T = \frac{1}{N}\sum_{i=1}^{N} \left\| T_i^{pred} - T_i^{True} \right\|^2, \; L_S = \frac{1}{N}\sum_{i=1}^{N} \left\| \sigma_i^{pred} - \sigma_i^{True} \right\|^2 \quad (4)$$

Here, T_i^{Pred} and σ_i^{Pred} denote the model predicted temperature and stress fields, T_i^{True} and σ_i^{True} the corresponding FEM reference fields. The weighting coefficients $\omega_T = 0.7$ and $\omega_S = 0.3$ are empirically chosen to balance thermal and mechanical accuracy.

To measure the prediction accuracy, the relative L² error is computed for each field and follows equation 5.

$$\varepsilon_{L2}(T) = \frac{\left\| T_i^{pred} - T_i^{True} \right\|^2}{\left\| T_i^{True} \right\|^2} \; and \; \varepsilon_{L2}(\sigma) = \frac{\left\| \sigma_i^{pred} - \sigma_i^{True} \right\|^2}{\left\| \sigma_i^{True} \right\|^2} \quad (5)$$

Lower L² errors indicate better agreement with the numerical reference and higher generalization of the surrogate model.

The validation is performed by comparing the model predictions with FEM reference solutions to verify accuracy and physical consistency across all parameter cases. This ensures that the trained model reliably reproduces the thermal and mechanical fields for the given process parameters.

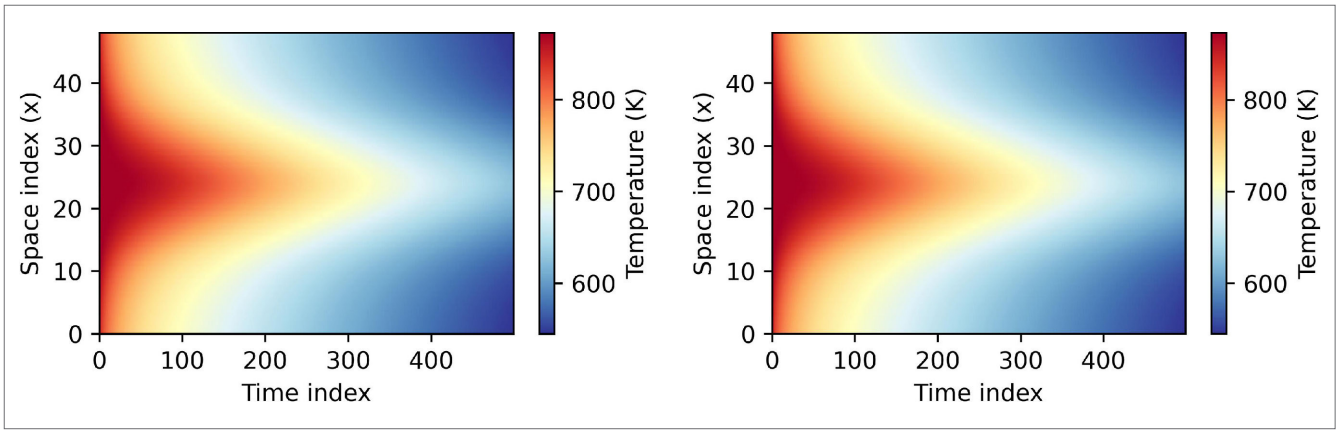

Figure 4 Visualization of temperature distributions predicted on seen dataset by the MIFNO model (left) and Finite Element Method (FEM) simulation (right) over 50 spatial nodes and 500-time steps during the cooling process of tempered glass, training performed over 2000 epochs. *Source: Universität Augsburg*

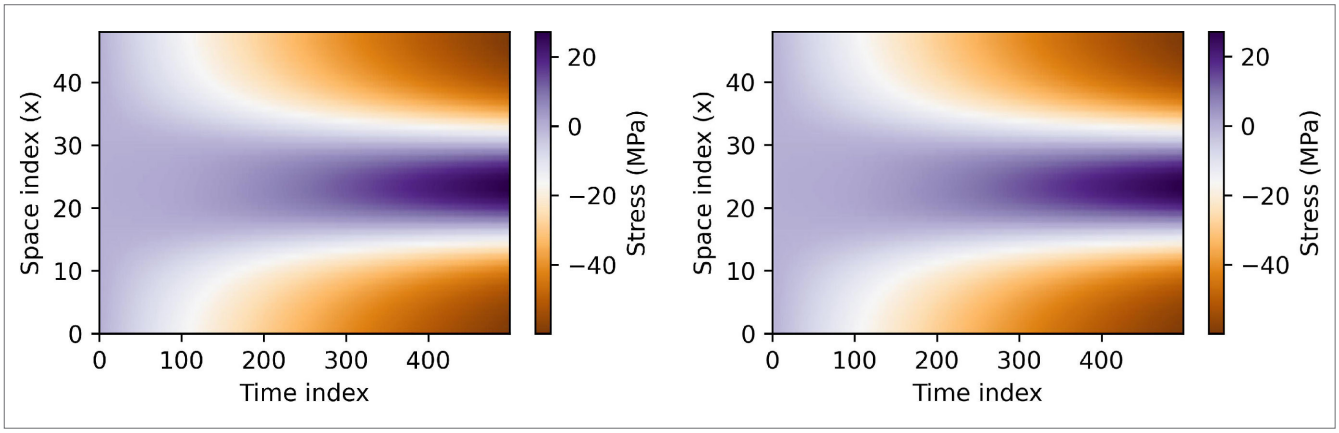

Figure 5 Visualization of residual stresses distributions predicted on seen dataset by the MIFNO model (left) and FEM simulation (right) over 50 spatial nodes and 500-time steps during the cooling process of tempered glass, training performed over 2000 epochs. *Source: Universität Augsburg*

3.5 Deployment and integration

The trained MIFNO model is deployed within an interactive visualization framework combining "FastAPI" and "Streamlit". FastAPI functions as a lightweight backend interference engine, loading pre-trained model weights and providing prediction endpoints for process parameters such as convective and radiative heat transfer coefficients [31]. It enables real-time interference of temperature and residual stress fields, updating predictions instantly as parameters change.

The Streamlit interface serves as the frontend layer, offering an intuitive control panel for parameter input, prediction visualization, and comparison with reference FEM data [32]. Results are displayed as dynamic spatial-temporal contour maps of temperature and stress, allowing users to explore the thermal-mechanical response interactively. This modular deployment architecture supports seamless integration within digital factory environments, enabling both independent simulations and web-based process monitoring and control applications.

4 Results

This section presents the validation of predicted temperature and residual stress fields obtained from the proposed Multi-Input Fourier Neural Operator (MIFNO) model against Finite Element Method (FEM) reference solutions. Comparisons are conducted along the 1D glass model consisting of 50 nodes and over 500 simulation time steps. The evaluation focuses on two main aspects of computational efficiency: generalization accuracy and computational time.

4.1 Generalization accuracy

4.1.1 Test on seen/trained dataset

The following figures compare the predicted temperature fields and residual stress distributions of the MIFNO model with the corresponding FEM reference results, respectively. A strong agreement is observed between both models, where MIFNO successfully reproduces the characteristic cooling pattern and parabolic stress distribution across the glass width.

For temperature prediction, as shown in **figure 4**, the model demonstrates excellent agreement with the initial temperature distribution, the boundary conditions, and the gradual cooling trend toward the central region. The following process parameters are used, as convective heat transfer is 100 $Wm^{-2}\,K^{-1}$, emissivity is 0.85, *Stefan Boltzmann* constant is 5.67e-8 $Wm^{-2}K^{-4}$ and thermal diffusivity is 15.

Similarly, for residual stresses, the predicted compressive and tensile regions correspond closely to the FEM solution, as presented in **figure 5**. During the initial cooling stage (up to approxi-

Table 1 Generalization performance of MIFNO with different dataset sizes over 1000 epochs.

Datasets	16 use cases	81 use cases
L^2 error for temperatures	0.2784 %	0.1233 %
L^2 error for stresses	0.7454 %	0.2485 %

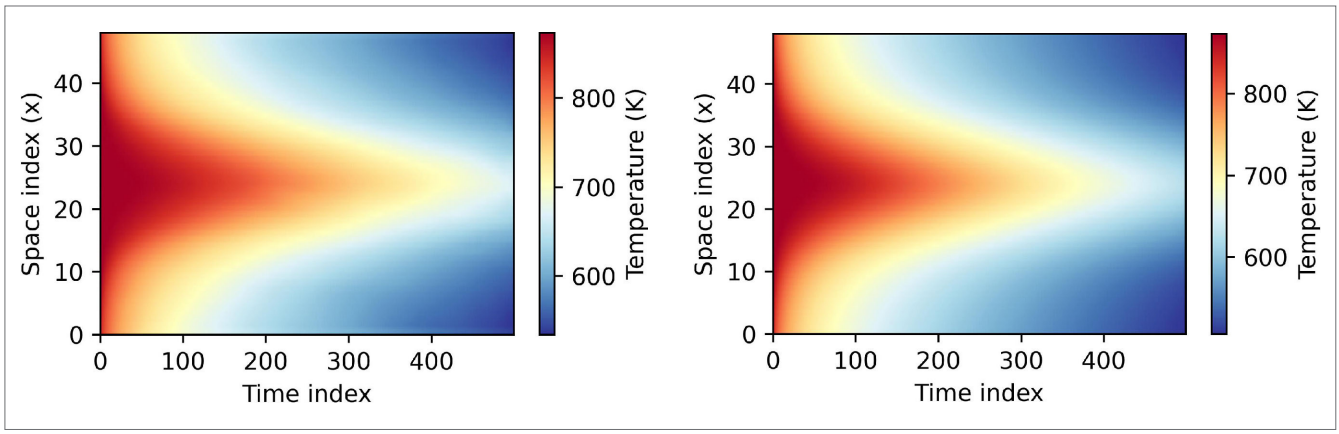

Figure 6 Visualization of temperature distributions predicted on unseen dataset by the MIFNO model (left) and FEM simulation (right) over 50 spatial nodes and 500-time steps during the cooling process of tempered glass, training performed over 2000 epochs. *Source: Universität Augsburg*

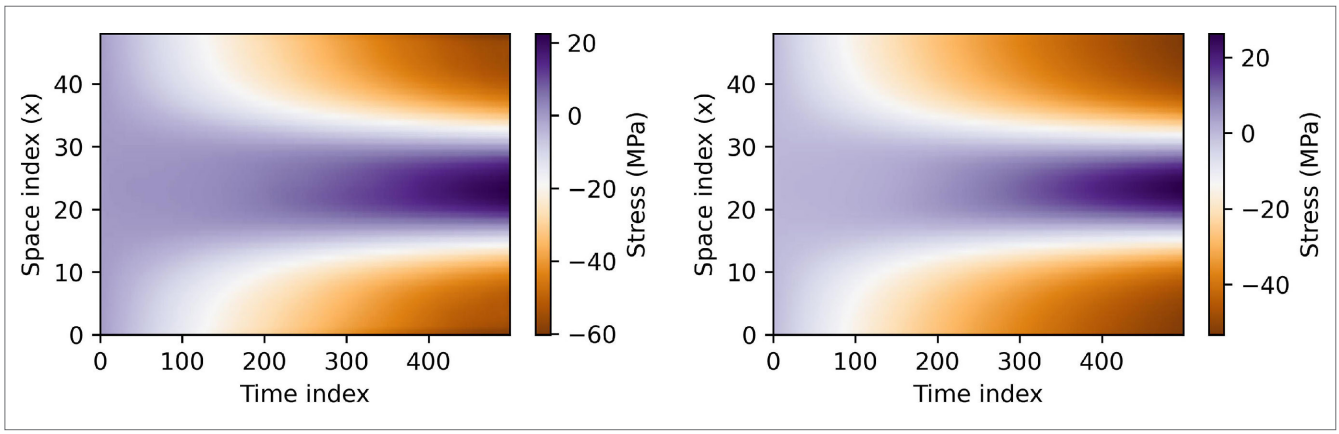

Figure 7 Visualization of residual stresses distributions predicted on unseen dataset by the MIFNO model (left) and FEM simulation (right) over 50 spatial nodes and 500-time steps during the cooling process of tempered glass, training performed over 2000 epochs. *Source: Universität Augsburg*

mately 100 seconds), tensile stresses dominate across the glass width. With further cooling, the compressive stresses begin to develop at the boundaries, while tensile stresses remain concentrated in the central region, leading to an overall stress equilibrium characteristic of the tempered glass state.

Quantitatively, MIFNO achieved a mean relative L^2 error of 0.029 % for temperature fields and 0.078 % for residual stresses, highlighting its strong generalization ability across all parameterized cases without overfitting to specific boundary or process conditions.

4.1.2 Influence of dataset size

When the dataset was expanded from 16 to 81 use cases, the model's generalization improved further, even with a reduced training duration of 1000 epochs, as summarised in **table 1**.

4.1.3 Test on unseen dataset

The following figures illustrate the temperature and stress distributions predicted for an unseen set of process parameters not included in the training dataset. The following variables were applied and compared with corresponding FEM simulations: convective heat transfer is 135 $W.m^{-2}$ K^{-1}, emissivity is 0.69, *Stefan Boltzmann* constant is 3.30e-8 $W.m^{-2}K^{-4}$ and thermal diffusivity is 11.

For the following temperature predictions in **figure 6**, the MIFNO model captures the overall cooling trend but shows slight deviations in the central region, where predicted temperatures remain around 700 K even after 400 s, unlike the temperature values from FEM predictions.

As demonstrated in **figure 7**, the following stress distribution indicates that the onset of compressive stresses is delayed in the MIFNO predictions compared to the FEM results. In the MIFNO case, compressive stresses emerge at approximately 150 s, whereas in the FEM reference they appear earlier, around 100 s.

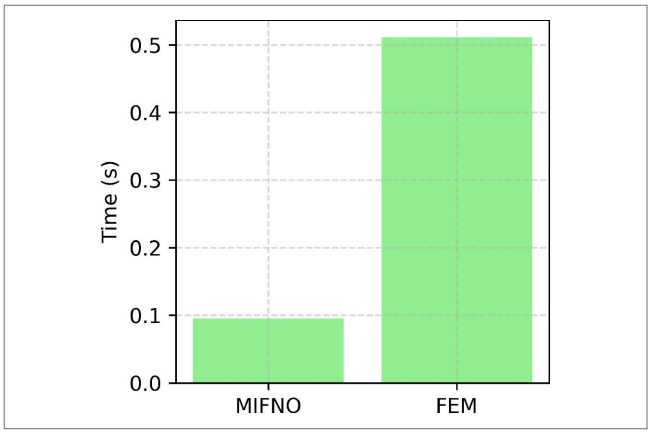

Figure 8 Interference time comparison between MIFNO and FEM for the seen dataset over 2000 epochs. *Source: Universität Augsburg*

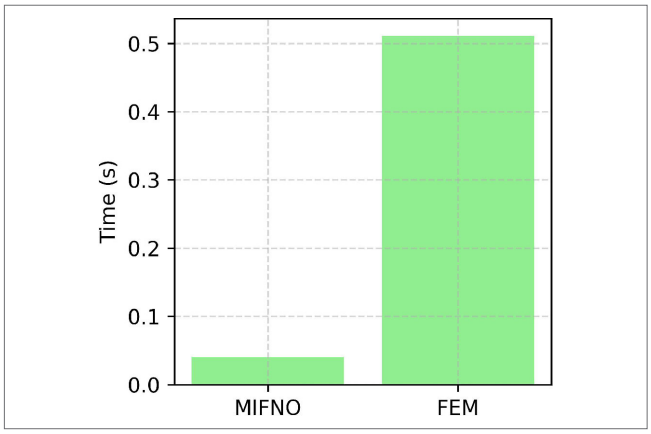

Figure 9 Interference time comparison between MIFNO and FEM for the unseen dataset over 2000 epochs. *Source: Universität Augsburg*

Table 2 Training and interference times of MIFNO for different sizes over 1000 epochs.

Datasets	16 use cases	81 use cases
Training time	4113.64s	61429.24 s
Interference time	0.096954s	0.067483s

Quantitatively, MIFNO achieved a mean relative L^2 error of 3.496 % for temperature fields and 6.234 % for residual stresses, highlighting its fair generalization ability across all parameterized cases without overfitting to specific boundary or process conditions.

4.2 Computational time

4.2.1 Test on seen/trained dataset

Computational efficiency is evaluated based on training, interference, and reference simulation times. While the FEM simulation requires 0.69 s per case to compute both thermal and mechanical fields, MIFNO performs the same prediction in only 0.09 s, as shown on the following **figure 8**. On the other side, the training of the model requires 9464 s to perform over 2000 epochs on all 16 use cases.

4.2.2 Influence of dataset size

When the dataset size was increased to 81 cases, the total training time rose substantially due to the larger parameter space, but the interference time per sample decreased significantly, as summarized in **table 2**. Training of models is performed in that comparison over only 1000 epochs.

4.2.3 Test on unseen/untrained dataset

For unseen parameter combinations, the MIFNO model continues to show outstanding computational efficiency. While the FEM simulation requires 0.69 s per case, MIFNO predicts the same thermal and mechanical fields in only 0.046 s, as observed on **figure 9**. The total training time for this model configuration is approximately 6334.88 s over 2000 epochs on all 16 use cases.

5 Conclusion and outlook

The results demonstrate a significant increase in computational efficiency of the developed MIFNO model compared to the numerical FEM simulation, while maintaining strong accuracy and flexibility across different process parameters, especially on seen parameters. This flexibility allows the model to act as a fully independent, parameterized surrogate solver, capable of producing efficient and consistent solutions under varying boundary and material conditions.

Expanding the training dataset from 16 to 81 use cases would further enhance the model's smoothness and robustness, although training time of the model is sharply increased. Moreover, such enrichment of the dataset with additional operational variables is expected to reduce interference time per case and broaden the model's generalization capability.

A remarkable 7.7× speed-up (-87 % runtime) and 15× speed-up (-93 % runtime) were achieved in interference time on seen and unseen process parameters, respectively, confirming the model's suitability for real-time process simulations, even for high-dimensional or fine-mesh problems. Although the total training time is relatively high due to iterative optimization over 2000 epochs, this computational cost is incurred only once during model preparation. Once trained, the MIFNO model can generalize to unseen process parameters without any need for additional meshing or iterative solving.

Beyond efficiency improvements, the MIFNO framework offers continuous field predictions that are independent of the spatial or temporal discretization used in FEM. This property enables adaptive evaluation under arbitrary process settings, such as varying convective or radiative heat transfer coefficients and different initial temperatures.

Due to its fast-response capability and parameterized nature, the MIFNO model represents a promising foundation for digital twin integration, online process monitoring, and optimization applications in glass manufacturing and other industrial processes

FUNDING NOTES

This work was funded by "Bayerisches Staatsministerium für Wirtschaft, Landesentwicklung und Energie" under project titled "Surroglas".

ACKNOWLEDGEMENTS

We would like to thank the "Bayerisches Staatsministerium für Wirtschaft, Landesentwicklung und Energie (StMWi)" for the financial support and for enabling this research, which contributes to the digital and sustainable transformation of industrial value-creation systems.

REFERENCES

[1] Moradinia, Z.; Vandierendonck, H.; Murphy, A.: Navigating speed–accuracy trade-offs for multi-physics simulations. Meccanica 60 (2025), pp. 1583–1599

[2] Soulaïmani, A.; Ben Haj Ali, A.; Feng, Z.: A parallel-distributed approach for multi-physics problems with application to computational nonlinear aeroelasticity. Canadian Aeronautics and Space Journal 50 (2004) 4, pp. 221–235

[3] Zimbrod, P.; Fleck, M.; Schilp, J.: An application-driven method for assembling numerical schemes for the solution of complex multiphysics problems. Applied System Innovation 7 (2024) 3, #35, https://doi.org/10.3390/asi7030035

[4] Meena, K. S.; Suriya, S.: A survey on supervised and unsupervised learning techniques. In: Kumar, L.; Jayashree, L.; Manimegalai, R. (Hrsg.): Proceedings of the International Conference on Artificial Intelligence, Smart Grid and Smart City Applications AISGSC, 2019, https://doi.org/10.1007/978-3-030-24051-6_58

[5] Hildebrand, S.; Klinge, S.: Comparison of neural FEM and neural operator methods for applications in solid mechanics. Neural Computing and Applications 36 (2024), pp. 16657–16682

[6] Cai, S.; Mao, Z.; Wang, Z. et al.: Physics-informed neural networks (PINNs) for fluid mechanics: a review. Acta Mechanica Sinica 37 (2021), pp. 1727–1738

[7] Blechschmidt, J.; Ernst, O. G.: Three ways to solve partial differential equations with neural networks—A review. GAMM-Mitteilungen 44 (2021) 2, e202100006

[8] Azizzadenesheli, K.; Kovachki, N.; Li, Z. et al.: Neural operators for accelerating scientific simulations and design. Nature Reviews Physics 6 (2024), pp. 320–328

[9] Peng, W.; Qin, S.; Yang, S. et al.: Fourier neural operator for real-time simulation of 3D dynamic urban microclimate. Building and Environment 248 (2024), #111063

[10] Burark, P.; Tiwari, K.; Rashid, M. M. et al.: CoDBench: A critical evaluation of data-driven models for continuous dynamical systems. Digital Discovery 3 (2024) 6, pp. 1172–1181

[11] Li, Z.; Kovachki, N.; Azizzadenesheli, K. et al.: Fourier neural operator for parametric partial differential equations. arXiv 2020, arxiv.org/abs/2010.08895

[12] Nielsen, J. H.; Olesen, J. F.; Poulsen, P. N. et al.: Finite element implementation of a glass tempering model in three dimensions. Computers & Structures 88 (2010) 17–18, pp. 963–972

[13] Kong, J.; Kim, J. H.; Chung, K.: Residual stress analysis with improved numerical methods for tempered plate glasses based on structural relaxation model. Metals and Materials International 13 (2007), pp. 67–75

[14] Nilpueng, K.; Kaseethong, P.; Mesgarpour, M. et al.: A novel temperature prediction method without using energy equation based on physics-informed neural network (PINN): A case study on plate-circular/square pin-fin heat sinks. Engineering Analysis with Boundary Elements 145 (2022), pp. 404–417

[15] Bowman, B.; Oian, C.; Kurz, J. et al.: Physics-informed neural networks for the heat equation with source term under various boundary conditions. Algorithms 16 (2023) 9, #428, HYPERLINK, https://doi.org/10.3390/a16090428

[16] He, Z.; Ni, F.; Wang, W. et al.: A physics-informed deep learning method for solving direct and inverse heat conduction problems of materials. materialstoday Communications 28 (2021), #102719

[17] Haghighat, E.; Raissi, M.; Moure, A. et al.: A deep learning framework for solution and discovery in solid mechanics. arXiv 2020, arxiv.org/abs/2003.02751

[18] Kafkas, P.; Giannakopoulos, G.; Rekatsinas, C.: Solving linear elasticity problems using physics-informed neural networks. Proceedings of the 13th Hellenic Conference on Artificial Intelligence, 2024, #50, https://doi.org/10.1145/3688671.3688746

[19] Yamazaki, Y.; Harandi, A.; Muramatsu, M. et al.: A finite element-based physics-informed operator learning framework for spatiotemporal partial differential equations on arbitrary domains. Engineering with Computers 41 (2025), pp. 1–29

[20] Rezaei, S.; Moeineddin, A.; Kaliske, M. et al.: Integration of physics-informed operator learning and finite element method for parametric learning of partial differential equations. arXiv 2024, arxiv.org/abs/2401.02363

[21] Hildebrand, S.; Klinge, S.: Comparison of neural FEM and neural operator methods for applications in solid mechanics. Neural Computing and Applications 36 (2024), pp. 16657–16682

[22] Lanthaler, S.; Stuart, A. M.: The parametric complexity of operator learning. IMA Journal of Numerical Analysis (2025), draf028, https://doi.org/10.1093/imanum/draf028

[23] Yuan, J.; Zeng, L.; Gui, Y.: Method for predicting conductive heat transfer topologies based on Fourier neural operator. International Communications in Heat and Mass Transfer 160 (2025), #108332

[24] Lehmann, F.; Gatti, F.; Clouteau, D.: Multiple-input Fourier neural operator (MIFNO) for source-dependent 3D elastodynamics. Journal of Computational Physics 527 (2025), #113813

[25] Xiao, S.; Jin, P.; Tang, Y.: Learning solution operators of PDEs defined on varying domains via MIONet. arXiv 2024, arxiv.org/abs/2402.15097

[26] Agboka, K.; Béchet, F.; Siedow, N. et al.: Influence of radiative heat transfer model on the computation of residual stresses in glass tempering process. International Journal of Applied Glass Science 9 (2018) 2, pp. 235–251

[27] Aronen, A.; Karvinen, R.: Effect of glass temperature before cooling and cooling rate on residual stresses in tempering. Glass Structures & Engineering 3 (2018), pp. 3–15

[28] Çengel, Y. A.; Ghajar, A. J.: Heat and Mass Transfer: Fundamentals and Applications. New York: McGraw-Hill Education 2024

[29] Markovsky, A.; Soules, T. F.; Boyd, D. C.: An efficient and stable algorithm for calculating fictive temperatures. Journal of the American Ceramic Society 67 (1984) 4, pp. c56–c57

[30] Bergman, T. L.; DeWitt, D. P.; Incropera, F. P. et al.: Fundamentals of Heat and Mass Transfer. Hoboken: John Wiley & Sons 2011

[31] FastAPI: Tutorial – User Guide. Internet: fastapi.tiangolo.com/tutorial/. Accessed: 28.01.2026

[32] Streamlit: Streamlit Documentation. Internet: docs.streamlit.io/. Accessed: 28.01.2026

Tarek Hussein, M.Sc.
tarek.hussein@uni-a.de

Prof. Dr.-Ing. Johannes Schilp
johannes.schilp@informatik.uni-augsburg.de

Universität Augsburg
Lehrstuhl für Ingenieurinformatik – Produktionsinformatik
Universitätsstr. 2, 86159 Augsburg